pharmaceuticals

MDPI

Article

Application of RP-18 TLC Retention Data to the Prediction of the Transdermal Absorption of Drugs

Anna W. Sobańska [1,*], Jeremy Robertson [2] and Elżbieta Brzezińska [1]

[1] Department of Analytical Chemistry, Faculty of Pharmacy, Medical University of Lodz, ul. Muszyńskiego 1, 90-151 Łódź, Poland; elzbieta.brzezinska@umed.lodz.pl
[2] Chemistry Research Laboratory, Department of Chemistry, University of Oxford, Mansfield Road, Oxford OX1 3TA, UK; jeremy.robertson@chem.ox.ac.uk
* Correspondence: anna.sobanska@umed.lodz.pl

Abstract: Several chromatographic parameters ($R_M{}^0$ and S obtained from RP-18 TLC with methanol—pH 7.4 phosphate buffer mobile phases by extrapolation to zero concentration of methanol; R_f and R_M obtained from RP-18 TLC with acetonitrile—pH 7.4 phosphate buffer 70:30 v/v as a mobile phase) and calculated molecular descriptors (molecular weight—M_W; molar volume—V_M; polar surface area—PSA; total count of nitrogen and oxygen atoms—(N+O); H-bond donor count—HD; H-bond acceptor count—HA; distribution coefficient—log D; total energy—E_T; binding energy—E_b; hydration energy—E_h; energy of the highest occupied molecular orbital—E_{HOMO}; energy of the lowest unoccupied orbital—E_{LUMO}; electronic energy—E_e; surface area—S_a; octanol-water partition coefficient—log P; dipole moment—DM; refractivity—R, polarizability—α) and their combinations (R_f/PSA, R_M/M_W, R_M/V_M) were tested in order to generate useful models of solutes' skin permeability coefficient log K_p. It was established that neither $R_M{}^0$ nor S obtained in the conditions used in this study is a good predictor of the skin permeability coefficient. The chromatographic parameters R_f and R_f/PSA were also unsuitable for this purpose. A simple and potentially useful, purely computational model based on (N+O), log D and HD as independent variables and accounting for *ca.* 83% of total variability was obtained. The evaluation of parameters derived from R_M (R_M, R_M/M_W, R_M/V_M) as independent variables in log K_p models proved that R_M/V_M is the most suitable descriptor belonging to this group. In a search for a reliable log K_p model based on this descriptor two possibilities were considered: a relatively simple model based on 5 independent variables: (N+O), log D, R_M/V_M, E_T and E_h and a more complex one, involving also E_b, M_W and PSA.

Keywords: skin permeation; thin layer chromatography; computational descriptors

Citation: Sobańska, A.W.; Robertson, J.; Brzezińska, E. Application of RP-18 TLC Retention Data to the Prediction of the Transdermal Absorption of Drugs. *Pharmaceuticals* **2021**, *14*, 147. https://doi.org/10.3390/ph14020147

Academic Editor: Jean Jacques Vanden Eynde
Received: 31 December 2020
Accepted: 7 February 2021
Published: 12 February 2021

1. Introduction

The skin is the heaviest organ in the human body. Its average surface area is ca. 2 m2 and it accounts for about $1/_{10}$ of the total bodyweight [1]. The skin provides a selective barrier, allowing transdermal delivery of drugs and providing protection against harmful chemicals. Topically applied drugs and other compounds enter the body via either the transepidermal pathway (diffusion across the skin layers) or the appendageal pathway (through hair follicles or sweat ducts), the latter being considered significantly less important [1]. In the transepidermal pathway the molecule permeates the skin either transcellularly or intercellularly and the preferred route depends on the solute's molecular properties—small hydrophilic molecules prefer the transcellular route and lipophilic ones favor the opposite [1]. The rate of drug permeation through skin is expressed as the flux (J)—the amount of substance permeated per unit area and unit time. The flux depends on the permeabilityof the skin to the permeant (K_p) and the gradient of permeant concentration across the skin(Δc): $J = K_p \cdot \Delta c$.

For passive diffusion, the permeability coefficient K_p depends on the partition coefficient P, the diffusion coefficient D and the diffusional pathlength h: $K_p = P \cdot D/h$.

The ability of compounds to cross the skin barrier is of great interest to pharmaceutical and medicinal chemists because the transdermal delivery of drugs is an effective alternative to systemic delivery. This ability is also important in the context of environmental toxicology, because many harmful substances enter the body through skin. Transdermal permeation of drugs may be studied using many methods, including in vitro experiments on excised human skin [2] but there are many problems connected with this methodology. Aside from ethical considerations, the compound's skin permeability may differ significantly between individuals, depending on age and race and even between skin samples taken from the same individual. Percutaneous absorption is therefore studied on other, more convenient, models, including pig, rabbit, rat, mouse or shed snake skin, cultured human skin cells, or synthetic membranes [2,3]. However, such models require much tedious experimental work, so alternative solutions have been sought. Skin permeation depends on some readily obtained physicochemical parameters of a molecule, including the well-established predictor of lipophilicity and biological activity of compounds, the partition coefficient between aqueous and organic layers log P_{ow} [4]. However, it was demonstrated that log P_{ow} cannot be applied as a single measure of log K_p across a very wide range of chemical families, so molecular weight or volume were incorporated as additional descriptors [5,6]. Further research supported a relationship between K_p and hydrogen bond donor and acceptor activity (H_d and H_a, respectively) [7] and a melting point M_{Pt} [8]. Other authors stressed the importance of solvation free energy [9]. Log K_p was also correlated with Abraham's solute descriptors [10–12]. Following QSAR studies on skin permeation, models involving log P_{ow} and M_w along with further descriptors were developed [13–15]. Different computational skin permeability models have been reviewed and compared [15–22], and the most interesting equations discussed there are presented in Table 1.

Table 1. Selected computational models of skin permeation.

Equation	*n*	*R*	Ref.
$\log k_p = -1.36\ \Delta\log P_{oct\text{-}hept} - 3.38$	21	0.90	[4]
$\log K_p = -6.3 + 0.71 \log P_{ow} - 0.0061\ M_w$	93	0.82	[6]
$\log K_p = 0.82 \log P_{ow} - 0.0093\ V_M - 0.039\ M_{Pt} - 2.36$	60	0.95	[8]
$\log K_p = 0.84 \log P_{ow} - 0.07\ (\log P_{ow})^2 - 0.27\ H_b - 1.84 \log M_w + 4.39$	22	0.98	[23]
$\log K_p = 0.652 \log P_{ow} - 0.00603\ M_w - 0.623\ ABSQon - 0.313\ SsssCH - 2.30$	143	0.95	[13]
$\log K_p = -5.426 - 0.106\ E - 0.473\ S - 0.473\ A - 3.000\ B + 2.296\ V$	119	0.91	[12]
$\log K_p = -3.05 - 0.0065\ QXXp + 0.65\ ALOGP - 1.75\ Neoplastic\text{-}80 + 0.22\ F06[C\text{-}N]$	158	0.91	[14]
$\log K_p = -5.426 - 0.106\ E - 0.473\ S - 0.473\ A - 3.000\ B + 2.296\ V$	119	0.91	[12]
$\log K_p = -5.048 - 0.586\ \pi_2{}^H - 0.633 \Sigma\alpha_2{}^H - 3.481\ \Sigma\beta_2{}^H + 1.787\ V$	46	0.98	[10]

Where: log P_{ow}—octanol-water partition coefficient; $\Delta\log P_{oct\text{-}hept}$—the difference between logarithms of octanol-water and heptane-water partition coefficients; M_W—molecular weight; V_M—molecular volume; M_{Pt}—melting point; *SsssCH*—sum of E-state indices for all methyl groups; *ABSQon*—sum of absolute charges on nitrogen and oxygen atoms; H_b—total H-bond count; *A*, *B*, *S*, *E*, *V*—Abraham's solvation parameters (*A*—hydrogen bond acidity; *B*—hydrogen bond basicity; *S*—dipolar interactions; *E*—excess molar refractivity; *V*—McGowan's characteristic volume); *Neoplastic-80*—antineoplastic-like property at 80% similarity; *ALOGP*—log P_{ow} calculated using ALOGP algorithm; *F06[C-N]*—frequency of carbon-nitrogen bond at a topological distance of 06; *QXXp*—electrostatic interactions between electric quadrupoles of van der Waals forces; $\pi_2{}^H$—solute dipolarity/polarizability; $\Sigma\alpha_2{}^H$—solute overall hydrogen-bond acidity; $\beta_2{}^H$—solute overall hydrogen bond basicity.

More recent developments in the field of in silico evaluation of skin permeability include the model proposed by Chenet et al., [24], in which predictions of skin permeability may be based on certain molecular properties and topological descriptors.

The equation proposed by Potts is among the most accurate and the most frequently cited of the computational models of skin permeability coefficient [21,22], although the model developed by Mitragotri [25] is also interesting [21]—supposedly giving even more reliable predictions—but the model by Potts has the benefit of simplicity.

Chromatography is a powerful technique for acquiring measurements of physicochemical and biological properties of solutes, including the ability of compounds to cross different biological barriers [26–28]. It is superior to techniques based on excised human skin, animal experiments or even cell cultures because it is more reproducible and it usually involves commercially available chromatographic supports. The chromatographic

techniques used to predict the skin permeability of solutes include normal- and reversed-phase thin layer chromatography [29,30], immobilized artificial membrane (IAM) column chromatography [31–34], RP-18 column chromatography [33–35], column chromatography on a novel stationary phase based on immobilized keratin [36], biopartitioning micellar chromatography (BMC) [37–39], micellar electrokinetic chromatography [34], and liposome electrokinetic chromatography [40]. Available models of skin permeability parameters, based on liquid chromatographic descriptors, are presented in Table 2.

Table 2. Selected relationships between skin permeability and liquid chromatographic descriptors.

	Equation	*n*	*R*	Reference
NP TLC	$\log K_p = -1.318 (R_M^0)^2 - 7.529 R_M^0 - 9.142$ (dioxane-cyclohexane)	7	0.98	[30]
	$\log K_p = -0.762 (R_M^0)^2 - 5.146 R_M^0 - 6.955$ (THF-cyclohexane)	7	0.97	
IAM HPLC	$\log K_p = -10.19 + 1.77 \log k^{IAM}$	10	0.94	[31]
	$\log K_{sc} = 0.40 + 0.64 \log k^{IAM}$	10	0.97	
	$\log K_p = -6.16 - 0.46 (\log k^{IAM})^2 + 1.54 \log k^{IAM}$	14	0.80	
	$\log K_p = -6.09 + 1.05 \log k^{IAM}$	14	0.88	
	$\log K_p = -5.154 + 1.443 \log k^{IAM}$	32	0.51	[33]
	$\log K_{sc} = 1.555 + 1.522 \log k^{IAM}$	15	0.92	
	$\log K_p = -5.09 + 1.94 \log k^{IAM}$	32	0.55	[34]
	$\log K_p = -3.58 + 2.56 \log k^{IAM} - 1.12 V$	32	0.86	
	$\log K_p = -2.419 \Delta\log k_w^{IAM} - 2.206$	10	0.95	[32]
	$\log K_p = -2.136 \Delta\log k_w^{IAM} + 0.037 \log P_{ow} - 2.373$	10	0.94	
	$\log K_p = -2.182 \Delta\log k_w^{IAM} + 0.046 \log k_w^{IAM} - 2.323$	10	0.94	
RP-18	$\log K_p = -4.76 + 1.44 \log k - 1.16 V$	27	0.91	[34]
	$\log K_p = -5.728 + 1.636 \log k$ (MSC18 column)	32	0.75	[33]
	$\log K_p = -5.865 + 1.849 \log k$(RP-18 column)	32	0.73	
	$\log K_{sc} = 1.131 + 0.855 \log k$ (MSC18 column)	15	0.87	
	$\log K_{sc} = 1.099 + 0.95 \log k$ (RP-18 column)	15	0.85	
BMC	$\log K_p = -3.3 + 1.3 \log k_{BMC} - 0.008 M_{Pt}$	42	0.91	[37]
	$\log K_p = -2.24 + 1.83 \log P_{mw} - 0.0123 M_w$	22	0.91	[39]
Keratin	$\log K_p = -6.558 + 1.920 \log k^{IAM} - 1.039 \log k_{KERATIN}$	17	0.93	[36]

Where: K_p—skin permeability coefficient; R_f—retention factor in thin layer chromatography; $R_M = \log (1/R_f - 1)$ and R_M^0 are obtained by extrapolation of R_M values from a series of TLC experiments conducted for different concentrations φ of a modifier in mobile phases to zero concentration of the modifier, according to the equation: $R_M = R_M^0 + S\varphi$; P_{mw}—micelle-water partitioning coefficient; k—retention factor in column liquid chromatography; k^{IAM}, k_{BMC}, $k_{KERATIN}$—retention factors in IAM, BMC and immobilized keratin chromatography, respectively; k_w^{IAM}—k^{IAM} measured at or extrapolated to purely aqueous conditions; $\Delta\log k_w^{IAM}$—the difference between log k_w^{IAM} measured and predicted on the basis of log P_{ow}; V—McGowan's characteristic volume; M_w—molecular weight; M_{Pt}—melting point; K_{sc}—human skin-water partition coefficient.

From the equations presented in Table 2, it can be concluded that skin permeability coefficient is connected with chromatographic parameters (log k or R_M^0 for column and thin layer chromatography, respectively) *via* linear or reverse parabolic relationships. Chromatographic retention parameters are used either as sole skin permeability predictors, or they are combined with additional descriptors (log P_{ow}, V, M_w or M_{Pt}).

The objective of this study was to examine the relationships between the skin permeability coefficient log K_p and different, RP-18 chromatography-derived descriptors and other physicochemical parameters for a large group of structurally unrelated compounds, mainly drugs.

2. Results and Discussion

2.1. General Considerations

The majority of compounds analyzed in this study are drugs, administered either orally or in the form of injections, and whose transdermal delivery, in certain cases, is of interest. On the other hand, some topically applied substances (e.g., cosmetic preservatives) may exhibit the unwanted ability to cross the skin barrier. The skin permeability coefficient (K_p) is an important parameter that helps in the assessment of compounds' epidermal permeability; however, the experimentally determined values of K_p are available for only a few drugs, within the studied group. For this reason it was decided that the models of

skin permeability involving thin layer chromatographic and calculated descriptors should be generated and validated using K_p values obtained *in silico* with the EpiSuite software (DERMWIN v. 2 module) (log K_p^{EPI}), recommended by the US Environmental Protection Agency [41] and, at a final stage of these investigations, tested on a sub-group of analyzed solutes whose experimental log K_p values could be found (log K_p^{exp}). The estimation methodology used by DERMWIN is based on the Equation (2), related to the Potts model:

$$\log K_p \text{ (cm/h)} = -2.80 + 0.66 \log P_{ow} - 0.0056 M_W \ (R^2 = 0.66) \quad (1)$$

The values of log K_p^{EPI} obtained using DERMWIN are given in Table 3.

Table 3. Reference, experimental and calculated values of log K_p.

		log K_p^{EPI}	log $K_p^{(6)}$	log $K_p^{(7)}$	log $K_p^{(8)}$	log $K_p^{(9)}$	log $K_p^{(10)}$	log $K_p^{(12)}$	log K_p^{exp}
1	Diazepam	−2.53	−1.99	−1.99	−1.94	−1.95	−2.02	−2.01	
2	Temazepam	−3.04	−2.68	−2.70	−2.63	−2.66	−2.77	−2.80	
3	Alprazolam	−3.13	−2.41	−2.39	−2.47	−2.43	−2.69	−2.82	
4	Medazepam	−1.39	−1.41	−1.41	−1.53	−1.54	−1.68	−1.67	
5	Bromazepam	−3.22	−2.71	−2.73	−2.64	−2.65	−3.17	−3.25	
6	Chlordiazepoxide	−2.87	−2.66	−2.68	−2.69	−2.73	−2.83	−2.84	
7	Midazolam	−1.75	−1.83	−1.82	−1.92	−1.97	−2.29	−2.30	
8	Oxazepam	−2.92	−2.90	−2.94	−2.70	−2.73	−2.80	−2.80	
9	Lorazepam	−3.02	−2.87	−2.91	−2.71	−2.74	−3.14	−3.22	
10	Lormetazepam	−3.20	−2.66	−2.68	−2.48	−2.53	−2.87	−2.87	
11	Clorazepate	−3.21	−3.16	−3.15	−2.95	−2.94	−2.94	−2.96	
12	Ibuprofen	−1.32	−1.74	−1.80	−1.69	−1.66	−1.23	−1.14	−1.44 [9]
13	Zolpidem	−1.97	−2.32	−2.29	−2.41	−2.47	−2.24	−2.10	
14	Tamoxifen	−0.70	−0.87	−0.80	−0.89	−0.89	−0.61	−0.51	
15	Propranolol	−1.95	−2.42	−2.48	−2.41	−2.46	−2.25	−2.18	
16	Ranitidine	−4.39	−4.12	−4.09	−4.62	−4.58	−4.62	−4.83	−4.05 [9]
17	Methyldopa	−5.18	−4.27	−4.41	−4.58	−4.70	−4.66	−4.67	
18	Amizepin	−2.50	−2.49	−2.56	−2.29	−2.29	−2.36	−2.38	
19	Enalapril	−4.87	−3.93	−3.88	−4.74	−3.65	−4.94	−2.55	
20	Paracetamol	−3.35	−2.85	−2.97	−3.27	−3.34	−3.40	−3.41	
21	Aspirin	−3.03	−2.84	−2.88	−3.17	−3.21	−3.07	−3.00	−2.14 [9]
22	Cefuroxime	−5.29	−6.45	−6.33	−6.00	−6.03	−5.56	−5.38	
23	Theophylline	−3.84	−3.76	−3.77	−3.86	−3.84	−3.69	−3.63	
24	Verapamil	−2.84	−3.14	−3.06	−3.14	−3.27	−2.93	−2.80	
25	Clobazam	−3.08	−2.55	−2.56	−2.58	−2.64	−2.81	−2.79	
26	Mitrazapin	−2.28	−2.14	−2.17	−2.22	−2.27	−2.17	−2.11	
27	Promazine	−1.38	−1.68	−1.73	−1.76	−1.82	−1.71	−1.62	
28	Phenytoin	−2.58	−2.87	−2.91	−2.69	−2.69	−2.50	−2.46	
29	Hydroxyzine	−3.34	−2.71	−2.74	−2.62	−2.72	−2.86	−2.89	
30	Mianserin	−1.47	−1.66	−1.71	−1.74	−1.80	−1.73	−1.67	
31	Valproic acid	−1.79	−2.30	−2.43	−2.27	−2.30	−1.90	−1.83	
32	Zopiclone	−3.97	−4.10	−4.00	−4.13	−4.21	−4.25	−4.14	
33	Haloperidol	−2.06	−2.35	−2.40	−2.08	−2.24	−2.28	−2.19	
34	Risperidone	−2.79	−3.15	−3.07	−3.07	−3.18	−2.94	−2.79	
35	Loperamide	−2.06	−2.48	−2.47	−2.14	−2.29	−2.21	−2.11	
36	Phenylbutazone	−2.44	−2.78	−2.82	−2.73	−2.84	−2.66	−2.57	
37	Clonidine	−3.04	−2.80	−2.91	−2.63	−2.68	−3.16	−3.25	
38	PABA	−3.02	−3.38	−3.57	−3.22	−3.26	−3.09	−3.11	
39	Propylparaben	−1.80	−2.23	−2.27	−2.35	−2.31	−2.06	−2.05	
40	Methylparaben	−2.36	−2.39	−2.45	−2.61	−2.57	−2.44	−2.47	−2.04 [8]
41	Quetiap Quetiapine	−3.67	−3.14	−3.14	−3.11	−3.19	−3.09	−3.07	
42	Chlorprotixen	−1.13	−1.06	−1.10	−1.09	−1.14	−1.25	−1.20	
43	Perazine	−2.05	−1.96	−1.96	−1.93	−1.99	−1.84	−1.74	
44	Trifluoperazine	−1.75	−1.79	−1.77	−1.58	−1.73	−1.79	−1.65	
45	Thioridazine	−0.96	−1.48	−1.50	−1.44	−1.52	−1.27	−1.09	
46	Fluconazole	−4.19	−4.00	−3.96	−4.00	−4.04	−4.21	−4.24	
47	Tolperisone	−1.76	−1.74	−1.80	−1.75	−1.82	−1.45	−1.28	
48	Fenspiride	−2.75	−3.02	−3.09	−2.91	−3.00	−2.75	−2.66	
49	Pizotifen	−1.00	−1.04	−1.09	−1.08	−1.12	−0.87	−0.75	
50	Cyproheptadine	−1.30	−0.99	−1.02	−1.05	−1.08	−0.93	−0.86	
51	Clozapine	−2.52	−2.91	−2.96	−2.69	−2.79	−2.99	−2.97	
52	Tiapride	−4.05	−3.96	−3.99	−3.77	−3.91	−3.66	−3.51	
53	Olanzapine	−2.56	−2.61	−2.62	−2.50	−2.52	−2.34	−2.25	
54	Betahistine	−3.12	−2.66	−2.84	−2.68	−2.75	−2.66	−2.66	
55	Dexketoprofen	−2.16	−2.71	−2.82	−2.61	−2.70	−2.45	−2.37	
56	Caffeine	−3.94	−3.52	−3.50	−3.68	−3.68	−3.58	−3.51	−3.64 [34]
57	Hymecromone	−2.53	−2.66	−2.68	−2.89	−2.84	−2.77	−2.83	
58	Ketotifen	−1.99	−1.58	−1.62	−1.64	−1.71	−1.47	−1.32	
59	Clemastine	−1.09	−1.62	−1.66	−1.52	−1.63	−1.64	−1.57	
60	Salicylic acid	−2.08	−3.07	−3.22	−3.09	−3.10	−2.99	−3.05	−2.84 [9]
61	Indomethacin	−1.97	−3.40	−3.44	−3.24	−3.36	−3.49	−3.51	−3.67 [9,13]
62	Piroxicam	−2.63	−4.05	−4.00	−3.85	−3.84	−3.68	−3.65	−3.81 [9,13]
63	Naproxen	−1.98	−2.60	−2.69	−2.63	−2.68	−2.52	−2.54	−2.54 [37]

Where: log K_p^{exp}—experimental values; log K_p^{EPI}—values calculated using DERMWIN software; log $K_p^{(6)}$ to log $K_p^{(10)}$ and log $K_p^{(12)}$—values calculated according to Equations (6)–(10) and (12).

2.2. Thin Layer Chromatographic Parameters—Extrapolation Methodology

Reversed-phase thin layer chromatography has been used to predict physicochemical properties and bioavailability of compounds for many years [26] and the chromatographic parameter considered in these investigations is usually the R_M value defined by Bate-Smith and Westall (Equation (2)) [42]:

$$R_M = \log (1/R_f - 1) \quad (2)$$

The partitioning between chromatographic supports and an aqueous mobile phase resembles that between biomembranes and the aqueous phase. The most common approach to obtain the chromatographic retention parameters for water as a mobile phase is by using a series of chromatographic experiments with mobile phases containing different concentrations φ of a water-miscible solvent (organic modifier). Plots of R_M vs. φ are extrapolated to zero concentration of the modifier to furnish R_M^0 and the most common method to do so is by using the linear Soczewiński-Wachmeister Equation (3) [43].

$$R_M = R_M{}^0 + S \cdot \varphi \quad (3)$$

Apart from the R_M^0 value, other useful chromatographic descriptors derived from the linear extrapolation of R_M to purely aqueous conditions are the slope S and $C_0 = -R_M^0/S$.

The compounds **1** to **22** and **62** were chromatographed on the RP-18 stationary phase using methanol—pH 7.4 buffer mobile phases as described in Section 3. The values of R_M were calculated and plotted against the organic modifier concentration φ. The chromatographic parameters R_M^0 and S obtained according to Equation (3) (Table 4) were correlated with the log $K_p{}^{EPI}$ values presented in Table 3, and the resulting correlations were found to be unsatisfactory. Neither R_M^0 nor S correlated with log $K_p{}^{EPI}$ for the whole group of 23 compounds. 14 compounds (**2**, **3**, **5**, **6**, **8**, **9**, **10**, **11**, **16**, **17**, **18**, **20**, **21**, **62**) gave reverse parabolic relationships with R_M^0 and S (Figure 1), but the remaining solutes did not fit any reasonable pattern.

Table 4. Chromatographic parameters for compounds **1** to **63**.

		R_f	R_f/PSA	R_M	R_M/M_W	R_M/V_M	$R_M{}^0$	S
1	Diazepam	0.33	0.0101	0.308	0.00108	0.00123	3.578	−4.176
2	Temazepam	0.50	0.0095	0.000	0.00000	0.00000	3.050	−3.798
3	Alprazolam	0.22	0.0058	0.550	0.00178	0.00204	3.254	−3.877
4	Medazepam	0.56	0.0359	−0.105	−0.00039	−0.00042	2.528	−3.035
5	Bromazepam	0.51	0.0094	−0.017	−0.00005	−0.00007	2.496	−3.269
6	Chlordiazepoxide	0.62	0.0117	−0.213	−0.00070	−0.00079	2.131	−2.551
7	Midazolam	0.58	0.0230	−0.140	−0.00043	−0.00051	2.235	−2.741
8	Oxazepam	0.60	0.0097	−0.176	−0.00061	−0.00073	2.864	−3.752
9	Lorazepam	0.61	0.0099	−0.194	−0.00060	−0.00076	3.031	−4.037
10	Lormetazepam	0.49	0.0093	0.017	0.00005	0.00006	3.303	−4.207
11	Clorazepate	0.47	0.0060	0.052	0.00017	0.00020	3.117	−3.840
12	Ibuprofen	0.46	0.0122	0.078	0.00038	0.00037	4.139	−4.895
13	Zolpidem	0.68	0.0181	−0.327	−0.00106	−0.00109	1.744	−2.341
14	Tamoxifen	0.48	0.0381	0.043	0.00012	0.00015	5.041	−5.908
15	Propranolol	0.82	0.0198	−0.659	−0.00254	−0.00254	2.059	−3.004
16	Ranitidine	0.82	0.0074	−0.659	−0.00208	−0.00220	0.343	−0.518
17	Methyldopa	0.98	0.0094	−1.690	−0.00800	−0.00914	2.480	−0.197
18	Amizepin	0.55	0.0119	−0.087	−0.00033	−0.00040	2.484	−3.221
19	Enalapril	0.82	0.0085	−0.659	−0.00175	−0.00175	2.035	−2.994
20	Paracetamol	0.85	0.0172	−0.753	−0.00498	−0.00542	0.459	−1.500
21	Aspirin	0.76	0.0119	−0.501	−0.00278	−0.00328	1.301	−2.204
22	Cefuroxime	0.77	0.0039	−0.525	−0.00124	−0.00160	2.023	−3.307

Table 4. *Cont.*

		R_f	R_f/PSA	R_M	R_M/M_W	R_M/V_M	$R_M{}^0$	S
23	Theophylline	0.79	0.0114	−0.575	−0.00319	−0.00110		
24	Verapamil	0.77	0.0120	−0.525	−0.00115	−0.00036		
25	Clobazam	0.50	0.0124	0	0	0		
26	Mitrazapin	0.71	0.0366	−0.389	−0.00147	−0.00049		
27	Promazine	0.71	0.0223	−0.389	−0.00137	−0.00045		
28	Phenytoin	0.70	0.0120	−0.368	−0.00146	−0.00051		
29	Hydroxyzine	0.76	0.0212	−0.501	−0.00134	−0.00046		
30	Mianserin	0.77	0.1185	−0.525	−0.00199	−0.00065		
31	Valproic acid	0.54	0.1185	−0.070	−0.00048	−0.00013		
32	Zopiclone	0.80	0.1185	−0.602	−0.00155	−0.00059		
33	Haloperidol	0.78	0.0192	−0.550	−0.00146	−0.00053		
34	Risperidone	0.55	0.0089	−0.087	−0.00021	−0.00008		
35	Loperamide	0.53	0.0121	−0.052	−0.00011	−0.00004		
36	Phenylbutazone	0.39	0.0096	0.194	0.00063	0.00021		
37	Clonidine	0.83	0.0234	−0.689	−0.00299	−0.00110		
38	PABA	0.85	0.0134	−0.753	−0.00549	−0.00170		
39	Propylparaben	0.61	0.0131	−0.194	−0.00108	−0.00032		
40	Methylparaben	0.72	0.0155	−0.410	−0.00270	−0.00084		
41	Quetiapine	0.72	0.0098	−0.410	−0.00107	−0.00037		
42	Chlorprotixen	0.57	0.0200	−0.122	−0.00039	−0.00013		
43	Perazine	0.44	0.0126	0.105	0.00031	0.00011		
44	Trifluoperazine	0.44	0.0126	0.105	0.00026	0.00010		
45	Thioridazine	0.52	0.0091	−0.035	−0.00009	−0.00003		
46	Fluconazole	0.68	0.0095	−0.327	−0.00107	−0.00042		
47	Tolperisone	0.75	0.0369	−0.477	−0.00194	−0.00059		
48	Fenspiride	0.80	0.0178	−0.602	−0.00231	−0.00076		
49	Pizotifen	0.55	0.0175	−0.087	−0.00029	−0.00010		
50	Cyproheptadine	0.62	0.1914	−0.213	−0.00074	−0.00024		
51	Clozapine	0.68	0.0220	−0.327	−0.00100	−0.00035		
52	Tiapride	0.81	0.0096	−0.630	−0.00192	−0.00064		
53	Olanzapine	0.60	0.0102	−0.176	−0.00056	−0.00020		
54	Betahistine	0.72	0.0289	−0.410	−0.00301	−0.00079		
55	Dexketoprofen	0.61	0.0112	−0.194	−0.00076	−0.00025		
56	Caffeine	0.66	0.0123	−0.288	−0.00148	−0.00050		
57	Hymecromone	0.73	0.0157	−0.432	−0.00245	−0.00083		
58	Ketotifen	0.70	0.0144	−0.368	−0.00119	−0.00042		
59	Clemastine	0.45	0.0361	0.087	0.00025	0.00009		
60	Salicylic acid	0.70	0.0122	−0.368	−0.00266	−0.00088		
61	Indomethacin	0.46	0.0066	−0.069	0.000195	0.00007		
62	Piroxicam	0.50	0.0046	0	0	0	2.598	−3.193
63	Naproxen	0.59	0.0127	−0.158	−0.00069	−0.00022		

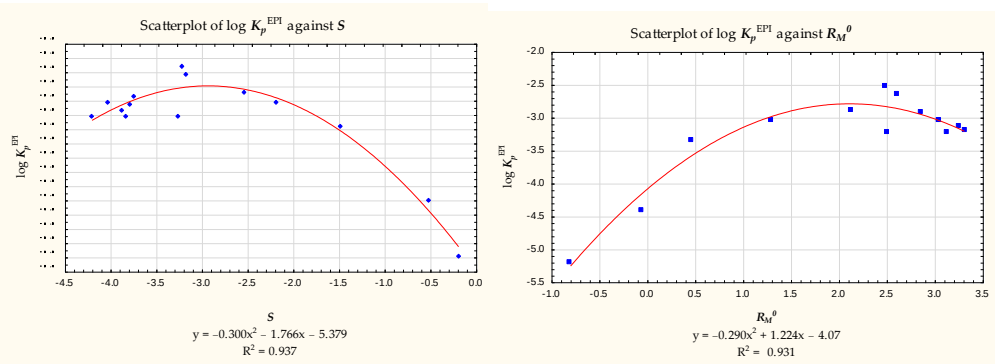

Figure 1. Scatterplots of log $K_p{}^{EPI}$ vs. S and $R_M{}^0$ (n = 14).

From this, it was evident that $\boldsymbol{R_M^0}$ and $\boldsymbol{S}$ obtained in the chromatographic conditions described in Section 3 could not be used as sole predictors of log $\boldsymbol{K_p}$. Attempts to generate a multivariate relationship between log $\boldsymbol{K_p}$ and the calculated physicochemical parameters, involving $\boldsymbol{R_M^0}$ or $\boldsymbol{S}$, failed and a purely computational model (4) was obtained by forward stepwise regression:

$$\log \boldsymbol{K_p} = 7.340\ (\pm 2.265) + 0.00018\ (\pm 0.00376)\ \boldsymbol{PSA} + 0.803\ (\pm 0.096)\ \log \boldsymbol{D} + 0.980\ (\pm 0.235)\ \boldsymbol{E_{HOMO}} - 0.959\ (\pm 0.184)\ \boldsymbol{E_{LUMO}} + 0.049\ (\pm 0.018)\ \boldsymbol{E_h} - 0.116\ (\pm 0.019)\ \boldsymbol{\alpha} \quad (4)$$
$$(n = 23,\ R^2 = 0.948,\ R^2_{adj.} = 0.928,\ F = 48.367,\ p < 0.00000,\ s_e = 0.316)$$

The same set of dependent variables was applied to compounds **1** to **60** to furnish the Equation (5) (Figure 2):

$$\log \boldsymbol{K_p} = -1.524\ (\pm 1.386) - 0.0176\ (\pm 0.0042)\ \boldsymbol{PSA} + 0.241\ (\pm 0.058)\ \log \boldsymbol{D} + 0.0149\ (\pm 0.140)\ \boldsymbol{E_{HOMO}} + 0.0472\ (\pm 0.189)\ \boldsymbol{E_{LUMO}} + 0.0311\ (\pm 0.0215)\ \boldsymbol{E_h} - 0.0113\ (\pm 0.0110)\ \boldsymbol{\alpha} \quad (5)$$
$$(n = 60,\ R^2 = 0.731,\ R^2_{adj.} = 0.700,\ F = 23.994,\ p < 0.00000,\ s_e = 0.572)$$

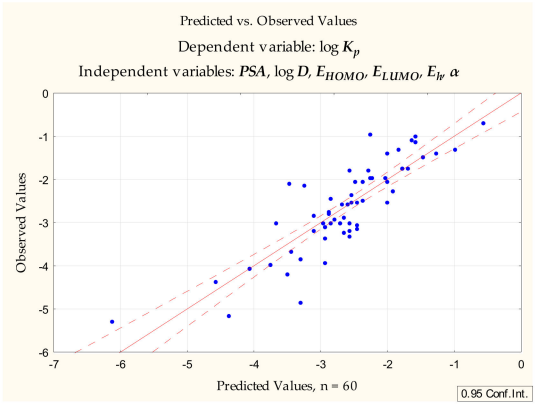

Figure 2. Equation (5)—predicted vs. observed values.

The Equations (4) and (5), based on the set of purely computational variables $\boldsymbol{PSA}$, log $\boldsymbol{D}$, $\boldsymbol{E_{HOMO}}$, $\boldsymbol{E_{LUMO}}$, $\boldsymbol{E_h}$ and $\boldsymbol{\alpha}$, are relatively simple and logical, since they involve some properties responsible for drug absorption (lipophilicity, polar surface area and polarizability) [44,45]. However, apart from poor statistics, the differences between the parameters of the Equations (4) and (5) suggest that they lack the required universality with respect to larger groups of structurally unrelated compounds.

2.3. Single Chromatographic Run Retention Parameters—R_f

The extrapolation method, although commonly used and recognized, has certain drawbacks. Several chromatographic experiments are required and the extrapolated $\boldsymbol{R_M^0}$ values depend on an organic modifier and its concentration range used to generate $\boldsymbol{R_M} = f(\boldsymbol{\varphi})$ plots. Some studies, therefore, use the single chromatographic run approach in which the $\boldsymbol{R_f}$ and $\boldsymbol{R_M}$ values are collected using a single concentration of an organic modifier in a mobile phase [46]. The single chromatographic run approach was used to predict the lipophilicity of selected cosmetic raw materials [47] and, in separate work, yielded two chromatographic descriptors, $\boldsymbol{R_f}$ and $\boldsymbol{R_f/PSA}$, used to study the blood-brain barrier permeation of solutes [48–50]. Apart from providing reliable lipophilicity descriptors, this methodology has additional advantages: it requires considerably less experimental work than any extrapolation or interpolation method, and none of the additional factors mentioned earlier (such as the modifier concentration range or the type of extrapolation curve) need to be taken into consideration.

Following the unsuccessful attempts to generate useful and universal models of the skin permeability coefficient using thin layer chromatographic retention parameters obtained by extrapolation ($\boldsymbol{R_M^0}$, $\boldsymbol{S}$), attention turned to the single RP-18 chromatographic

run approach developed in the earlier study of blood-brain barrier permeation [48–50]. The models presented in those studies involve $\boldsymbol{R_f}$ (collected as described in Section 3) and a novel parameter derived from it: $\boldsymbol{R_f/PSA}$. The latter (combined with $\boldsymbol{R_f}$ and a number of calculated physicochemical parameters) is a particularly good predictor of the blood-brain barrier permeability (expressed as steady state blood-brain partition ratio, log ***BB***). In the case of the skin permeability coefficient, however, this parameter (and $\boldsymbol{R_f}$ itself) failed to be selected in the course of the forward stepwise regression. The most interesting model (6) (Figure 3) generated at this stage of our investigations did not contain any chromatographic parameters and was as follows:

$$\log \boldsymbol{K_p} = -1.390\ (\pm 0.181) - 0.352\ (\pm 0.034)\ (\boldsymbol{N{+}O}) + 0.155\ (\pm 0.037) \log \boldsymbol{D} - 0.229\ (\pm 0.062)\ \boldsymbol{HD}$$
$$(n = 60,\ R^2 = 0.833,\ R^2_{adj.} = 0.824,\ F = 92.270,\ p < 0.0000,\ s_e = 0.438) \quad (6)$$

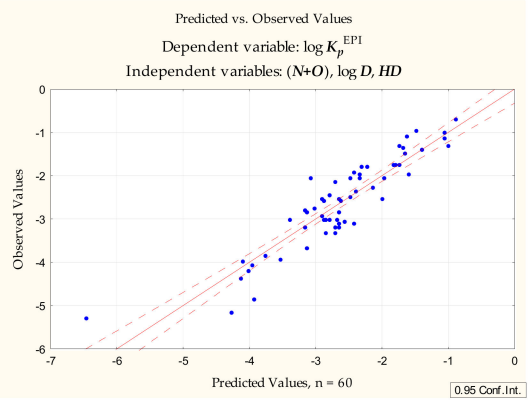

Figure 3. Equation (6)—predicted vs. observed values.

This model accounts for over 83% of total variability and contains the independent variables introduced in the following order: (***N+O***), log ***D***, ***HD***. The variables in the equation are strongly related to the conditions of good oral availability [44,45] and the ability to cross the blood-brain barrier [48–51]. The equation obtained at the very first stage of this regression, containing (***N+O***) as a sole independent variable, accounts for as much as 70% of total variability. The coefficients for (***N+O***) and ***HD*** are negative, which (as already observed, e.g., by Lien and Gaot [23]) suggests that excessive hydrogen bonding is an obstacle to epidermal permeability.

At this point the group of 60 studied compounds was divided into two subsets: a training set (**1** to **40**) and a test set (**41** to **60**).Equation (7) generated for the training set, and containing the same independent variables as Equation (6), was as follows:

$$\log \boldsymbol{K_p} = -1.561\ (\pm 0.248) - 0.319\ (\pm 0.041)\ (\boldsymbol{N{+}O}) + 0.177\ (\pm 0.053) \log \boldsymbol{D} - 0.256\ (\pm 0.072)\ \boldsymbol{HD}$$
$$(n = 40,\ R^2 = 0.819,\ R^2_{adj.} = 0.804,\ F = 54.356,\ p < 0.00000,\ s_e = 0.456) \quad (7)$$

The values of log $\boldsymbol{K_p}$ were calculated for compounds **41** to **60** according to Equation (7) and plotted against the reference log $\boldsymbol{K_p}^{EPI}$ values presented in Table 3. The linear relationship between these two groups of log $\boldsymbol{K_p}$ values improved when salicylic acid (**60**), whose $\boldsymbol{K_p}^{EPI}$ value seems to be overestimated compared to $\boldsymbol{K_p}^{exp}$ (due to the molecule's combined polarity and acidic properties, **60** is not a very good skin permeant), was removed as an outlier (R^2 = 0.83 and 0.89, respectively).

The model (6) was also tested on a subgroup of 9 compounds, analyzed in this study, whose log $\boldsymbol{K_p}^{exp}$ values were available (**12**, **16**, **21**, **40**, **56**, **60**, **61**, **62**, **63**). The resulting dependence is linear, with R^2 = 0.92, which is a much better result than that obtained for the relationship between log $\boldsymbol{K_p}^{exp}$ and log $\boldsymbol{K_p}^{EPI}$ (for n = 9, R^2 = 0.40).

2.4. Single Chromatographic Run Retention Parameters—$\boldsymbol{R_M}$

With the promising equations (6) and (7) in hand, attention turned to the possibility of using $\boldsymbol{R_M}$ values calculated from $\boldsymbol{R_f}$ obtained according to Section 3. Apart from $\boldsymbol{R_M}$

itself, other TLC-derived variables were tested: $\boldsymbol{R_M/V_M}$ and $\boldsymbol{R_M/M_W}$. The first model (8) involving $\boldsymbol{R_M}$–derived parameters, generated by forward stepwise multiple regression, was as follows (Figure 4):

$$\log \boldsymbol{K_p} = -1.651\ (\pm 0.185) - 0.370\ (\pm 0.034)\ (\boldsymbol{N{+}O}) + 0.130\ (\pm 0.034) \log \boldsymbol{D} + 90.44\ (\pm 43.04)\ (\boldsymbol{R_M/V_M}) - 0.0000058\ (\pm 0.0000019)\ \boldsymbol{E_T} + 0.0293\ (\pm 0.014)\ \boldsymbol{E_h} \quad (8)$$
$$(n = 60,\ R^2 = 0.868,\ R^2_{adj.} = 0.855,\ F = 70.869,\ p < 0.0000,\ s_e = 0.397)$$

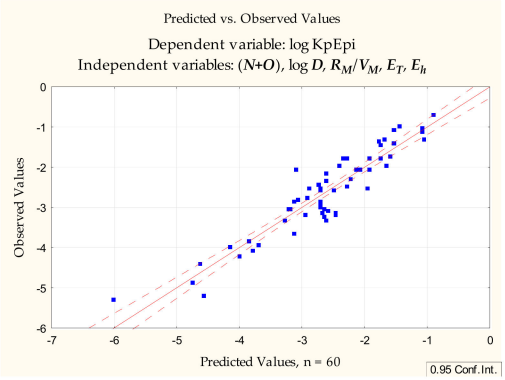

Figure 4. Equation (8)—predicted vs. observed values.

In Equation (8) the independent variables were introduced in the following order: $(\boldsymbol{N{+}O})$, log $\boldsymbol{D}$, $\boldsymbol{R_M/V_M}$, $\boldsymbol{E_T}$, $\boldsymbol{E_h}$. The difference between this model and Equation (6) was not very significant; $\boldsymbol{HD}$ was replaced with $\boldsymbol{R_M/V_M}$, and two more independent variables, responsible for a very small improvement in statistics, were introduced ($\boldsymbol{E_T}$, $\boldsymbol{E_h}$), but $(\boldsymbol{N{+}O})$ and log $\boldsymbol{D}$ still accounted for the greatest percentage of variability.

The group of 60 studied compounds was, as before, divided into a training set (**1** to **40**) and a test set (**41** to **60**). Equation (9), generated for the training set and containing the same independent variables as Equation (8), was as follows:

$$\log \boldsymbol{K_p} = -1.602\ (\pm 0.296) - 0.346\ (\pm 0.072)\ (\boldsymbol{N{+}O}) + 0.156\ (\pm 0.067) \log \boldsymbol{D} + 108.57\ (\pm 51.25)\ (\boldsymbol{R_M/V_M}) - 0.0000024\ (\pm 0.0000058)\ \boldsymbol{E_T} + 0.0254\ (\pm 0.0187)\ \boldsymbol{E_h} \quad (9)$$
$$(n = 40,\ R^2 = 0.823,\ R^2_{adj.} = 0.797,\ F = 31.654,\ p < 0.00000,\ s_e = 0.464)$$

Values of log $\boldsymbol{K_p}$ were calculated for compounds **41** to **60** according to Equation (9) and were plotted against the reference log $\boldsymbol{K_p}^{EPI}$ values. Just as in the case of Equation (7), the linear relationship between these two groups of log $\boldsymbol{K_p}$ values improved when salicylic acid (**60**) was removed as an outlier (R^2 = 0.87 and 0.92, respectively).

The model (8) was also tested on a subgroup of nine compounds, analyzed in this study, whose log $\boldsymbol{K_p}^{exp}$ values were available (**12**, **16**, **21**, **40**, **56**, **60**, **61**, **62**, **63**). The resulting relationship was linear, with R^2 = 0.80, which is a much better result than that obtained for the relationship between log $\boldsymbol{K_p}^{exp}$ and log $\boldsymbol{K_p}^{EPI}$ (for n = 9, R^2 = 0.40), but not as good as in the case of the Equation (6).

Equations (8) and (9) account for 87 and 82% of total variability, respectively, and have the advantage of being very simple; however, an attempt was made to improve their predictive abilities by adding further independent variables. Equation (10) (Figure 5) contains, apart from $(\boldsymbol{N{+}O})$, log $\boldsymbol{D}$ and $\boldsymbol{R_M/V_M}$ some more variables, $\boldsymbol{M_W}$ and $\boldsymbol{PSA}$, traditionally linked to good absorption properties, and it accounts for over 91% of total variability:

$$\log \boldsymbol{K_p} = -1.559\ (\pm 0.181) - 0.381\ (\pm 0.054)\ (\boldsymbol{N{+}O}) + 0.176\ (\pm 0.036) \log \boldsymbol{D} + 146.43\ (\pm 37.66)\ \boldsymbol{R_M/V_M} - 0.0000100\ (\pm 0.0000019)\ \boldsymbol{E_T} + 0.0469\ (\pm 0.014)\ \boldsymbol{E_h} - 0.0095\ (\pm 0.0020)\ \boldsymbol{M_W} - 0.00048\ (\pm 0.00011)\ \boldsymbol{E_b} + 0.0108\ (\pm 0.0037)\ \boldsymbol{PSA} \quad (10)$$
$$(n = 60,\ R^2 = 0.913,\ R^2_{adj.} = 0.899,\ F = 66.710,\ p < 0.0000,\ s_e = 0.332)$$

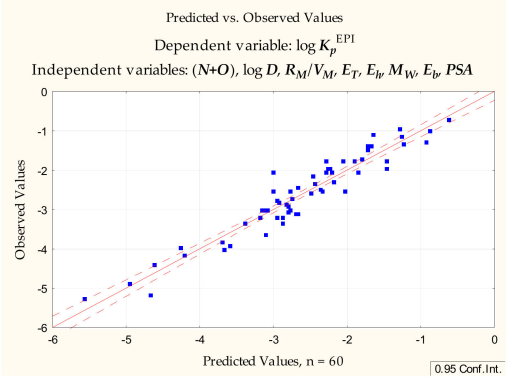

Figure 5. Equation (10), predicted vs. observed values.

The same set of variables as in Equation (10) was applied to the training set (compounds **1** to **40**). The Equation (11) generated at this stage was as follows:

$$\log \boldsymbol{K_p} = -1.426\ (\pm 0.283) - 0.398\ (\pm 0.130)\ (\boldsymbol{N{+}O}) + 0.157\ (\pm 0.063) \log \boldsymbol{D} + 168.41\ (\pm 51.99)\ \boldsymbol{R_M/V_M} - 0.0000327\ (\pm 0.0000221)\ \boldsymbol{E_T} + 0.0237\ (\pm 0.0204)\ \boldsymbol{E_h} - 0.0116\ (\pm 0.0046)\ \boldsymbol{M_W} - 0.000255\ (\pm 0.000189)\ \boldsymbol{E_b} + 0.00305\ (\pm 0.00813)\ \boldsymbol{PSA}$$
$$(n = 40,\ R^2 = 0.863,\ R^2_{adj.} = 0.827,\ F = 24.361,\ p < 0.0000,\ s_e = 0.428) \quad (11)$$

Equation (11) improved significantly after one compound (**19**) was removed. The difference between the $\boldsymbol{K_p}^{(11)}$ and $\boldsymbol{K_p}^{EPI}$ values for this compound is probably due to its very high energies and ***PSA***, coincidentally leading to overestimated skin permeability, calculated according to Equation (11):

$$\log \boldsymbol{K_p} = -1.590\ (\pm 0.185) - 0.399\ (\pm 0.084)\ (\boldsymbol{N{+}O}) + 0.178\ (\pm 0.041) \log \boldsymbol{D} + 138.00\ (\pm 34.01)\ \boldsymbol{R_M/V_M} - 0.000014\ (\pm 0.000015)\ \boldsymbol{E_T} + 0.067\ (\pm 0.015)\ \boldsymbol{E_h} - 0.012\ (\pm 0.003)\ \boldsymbol{M_W} - 0.000568\ (\pm 0.000131)\ \boldsymbol{E_b} + 0.014\ (\pm 0.006)\ \boldsymbol{PSA}$$
$$(n = 39,\ R^2 = 0.937,\ R^2_{adj.} = 0.921,\ F = 56.137,\ p < 0.0000,\ s_e = 0.278) \quad (12)$$

The values of log $\boldsymbol{K_p}$ were calculated for compounds **41** to **60** according to Equation (12) and plotted against the reference log $\boldsymbol{K_p}^{EPI}$ values. Just as in the case of Equation (9), the linear relationship between these two groups of log $\boldsymbol{K_p}$ values improved when salicylic acid (**60**) was removed as an outlier (R^2 = 0.831 and 0.886, respectively).

The model (10) was also tested on a subgroup of nine compounds, analyzed in this study whose log $\boldsymbol{K_p}^{exp}$ values were available (**12**, **16**, **21**, **40**, **56**, **60**, **61**, **62**, **63**). The resulting dependence was linear, with R^2 = 0.83, which is a much better result than that obtained for the relationship between log $\boldsymbol{K_p}^{exp}$ and log $\boldsymbol{K_p}^{EPI}$.

3. Materials and Methods

3.1. Chemicals

The 63 drugs analyzed during these investigations were isolated from pharmaceutical preparations, purchased from Sigma-Aldrich (St. Louis, MO, USA)or donated as free samples by Polfa-Pabianice (Pabianice, Poland). The purity of drugs isolated from pharmaceutical preparations was assessed by TLC and densitometry (Section 3). All isolated drugs gave single chromatographic spots (densitometric peaks) and were used without further purification. Drugs purchased from Sigma-Aldrich were of analytical or pharmacopeial grade. Distilled water used for chromatography was from an in-house distillation apparatus. Analytical grade acetonitrile and methanol were from Avantor Performance Materials Poland S.A. (formerly POCh S.A., Gliwice, Poland). pH 7.4 phosphate buffered saline was from Sigma-Aldrich.

3.2. Thin Layer Chromatography

Thin layer chromatography was performed on 10 × 20 cm glass-backed RP-18 F_{254s} TLC plates (layer thickness 0.25 mm) from Merck (Darmstadt, Germany). Before use, the plates were pre-washed with methanol-dichloromethane 1:1 (v/v) and dried overnight in ambient conditions. Solutions of compounds **1** to **63** in methanol (1 μg·μL^{-1}, spotting volume 1 μL), were spotted with a Hamilton microsyringe, 15 mm from the plate bottom edge, starting 10 mm from the plate edge, at 8 mm intervals. The chromatographic plates were developed in a vertical chromatographic chamber lined with filter paper and previously saturated with the mobile phase vapor for 20 min. The mobile phase consisted of acetonitrile—pH 7.4 phosphate buffered saline 70:30 (v/v) or methanol—pH 7.4 phosphate buffered saline (methanol contents from 90 to 50% v/v in 5% increments). The development distance was 95 mm from the plate bottom edge. After development, the plates were dried at room temperature and examined under UV light (254nm) and with a CD60 densitometer (Desaga, Germany, multiwavelength scan, 200–300 nm at 20 nm intervals). All chromatograms were repeated in duplicate, and the mean $\boldsymbol{R_f}$ values were used in further investigations. The chromatographic data are presented in Table 4.

3.3. Calculated Molecular Descriptors

The molecular descriptors for compounds investigated during this study were calculated with HyperChem 8.0, utilizing PM3 semi-empirical method with the Polak-Ribiere algorithm: total dipole moment—***DM*** [D], logarithm of the octanol-water partition coefficient—log ***P***, van der Waals molar volume—$\boldsymbol{V_M}$ [Å^3], surface area (grid and approximate)—$\boldsymbol{S_a}$ [Å^2], molecular weight—$\boldsymbol{M_w}$ [g mol^{-1}], energy of the highest occupied molecular orbital—$\boldsymbol{E_{HOMO}}$ [eV], energy of the lowest unoccupied molecular orbital—$\boldsymbol{E_{LUMO}}$ [eV], total energy—$\boldsymbol{E_T}$ [kcal mol^{-1}], binding energy—$\boldsymbol{E_b}$ [kcal mol^{-1}], electronic energy—$\boldsymbol{E_e}$ [kcal mol^{-1}], hydration energy—$\boldsymbol{E_h}$ [kcal mol^{-1}], refractivity—***R*** [Å^3], polarizability—$\boldsymbol{\alpha}$ [Å^3]. Other physicochemical parameters (distribution coefficient—log ***D***, polar surface area—***PSA*** [Å^2], H-bond donor count—***HD***, and H-bond acceptor count—***HA***) were calculated using ACD/Labs 8.0 software. The calculated molecular descriptors are given in Table 5. Statistical analysis was done using Statistica v.13 or StatistiXL v. 2.

Table 5. Calculated descriptors for compounds ***1*** to ***63***.

		PSA	*HD*	*HA*	log *D*	*N+O*	M_W	E_T	E_b	E_e	*DM*	E_{HOMO}	E_{LUMO}	$S_a(a)$	$S_a(g)$	V_M	E_h	log *P*	*R*	α
1	Diazepam	32.7	0	3	2.96	3	284.7	−69,868	−3697	−488,334	3.32	−9.20	−0.76	279.6	283.8	250.5	−2.75	0.94	87.8	31.0
2	Temazepam	52.9	1	4	2.20	4	300.7	−76,642	−3799	−541,464	3.98	−9.27	−0.87	289.2	291.9	257.1	−7.84	1.08	89.0	31.6
3	Alprazolam	38.1	0	4	2.50	4	308.8	−73,284	−3950	−550,378	6.48	−9.65	−1.23	293.7	299.4	269.4	−9.24	2.13	95.4	33.8
4	Medazepam	15.6	0	2	4.43	2	270.8	−63,807	−3705	−454,146	2.35	−8.82	−0.40	277.4	284.4	250.0	−1.58	1.75	88.1	30.9
5	Bromazepam	54.4	1	4	2.06	4	316.2	−67,922	−3290	−441,623	3.46	−9.33	−0.79	255.3	270.6	236.5	−5.68	−0.42	83.4	29.1
6	Chlordiazepoxide	53.1	1	4	2.36	4	301.8	−74,644	−3933	−566,228	1.88	−8.67	−0.31	304.6	304.2	268.3	−7.93	0.39	91.5	32.9
7	Midazolam	25.3	0	3	3.93	3	325.8	−82,444	−4091	−609,612	4.38	−9.17	−0.96	300.0	309.6	277.3	−3.37	0.13	98.4	34.4
8	Oxazepam	61.7	2	4	2.31	4	286.7	−73,199	−3524	−494,470	2.74	−9.13	−0.73	266.5	274.9	240.7	−7.92	0.84	84.1	29.8
9	Lorazepam	61.7	2	4	2.47	4	321.2	−80,151	−3508	−544,373	4.02	−9.28	−0.87	283.6	291.3	254.6	−9.96	0.61	88.8	31.7
10	Lormetazepam	52.9	1	4	2.36	4	335.2	−83,588	−3778	−599,987	1.93	−9.12	−0.64	307.2	308.3	271.7	−4.85	0.86	93.7	33.5
11	Clorazepate	78.8	2	5	2.90	5	314.7	−82,710	−3797	−581,135	3.32	−9.27	−0.93	288.7	293.6	258.0	−10.98	0.68	88.9	31.7
12	Ibuprofen	37.3	1	2	3.72	2	206.3	−55,498	−3380	−344,748	1.86	−9.51	0.06	262.5	251.3	210.1	−4.81	2.75	64.1	24.0
13	Zolpidem	37.6	0	4	3.07	4	307.4	−77,368	−4724	−613,528	4.07	−8.56	−0.55	355.6	351.1	300.7	−1.03	−0.22	99.6	35.9
14	Tamoxifen	12.5	0	2	7.88	2	371.5	−91,827	−6085	−810,401	0.59	−8.88	0.09	446.1	438.0	283.3	−2.55	2.88	131.6	46.2
15	Propranolol	41.5	2	3	3.10	3	259.4	−68,465	−4113	−472,868	1.26	−8.62	−0.43	311.9	307.7	259.4	−7.41	0.68	83.4	30.3
16	Ranitidine	111.6	2	7	1.23	7	316.4	−83,560	−4192	−562,535	3.41	−7.96	−0.21	403.6	378.1	299.3	−28.08	−4.02	89.1	33.6
17	Methyldopa	103.8	5	5	0.12	5	211.2	−62,797	−2902	−363,522	2.59	−9.03	−0.01	225.9	224.7	185.0	−21.50	−1.46	57.2	21.1
18	Amizepin	46.3	2	3	2.67	3	263.3	−59,477	−3441	−409,257	3.32	−9.01	−0.59	243.5	249.9	219.2	−6.48	−0.28	80.0	27.4
19	Enalapril	95.9	2	7	2.43	7	376.5	−102,647	−5843	−879,009	2.57	−8.94	0.28	421.3	441.2	376.5	−2.24	2.57	111.0	42.3
20	Paracetamol	49.3	2	3	0.34	3	151.2	−42,346	−2132	−207,000	4.31	−8.43	0.21	174.8	172.1	139.0	−10.61	−1.32	45.6	16.2
21	Aspirin	63.6	1	4	1.19	4	180.2	−54,523	−2335	−277,770	0.49	−9.66	−0.57	192.6	187.3	152.8	−7.43	−0.26	48.0	17.4
22	Cefuroxime	199.1	4	12	0.47	12	424.4	−122,720	−4706	−1,017,047	3.74	−9.47	−1.61	222.3	377.3	328.4	−18.43	−2.18	99.7	38.1
23	Theophylline	69.3	1	6	−0.20	6	180.2	−50,484	−2233	−281,145	3.47	−9.11	−0.57	301.7	335.5	523.0	−5.34	−1.31	45.1	17.0
24	Verapamil	64.0	0	6	2.33	6	454.6	−121,717	−7044	−1,150,691	3.64	−8.78	−0.95	705.7	817.4	1453.9	−8.35	2.81	136.6	51.5
25	Clobazam	40.6	0	4	1.59	4	300.7	−76,643	−3800	−546,998	0.55	−8.68	−0.23	402.3	486.0	813.3	−3.41	−1.40	89.7	31.5
26	Mitrazapin	19.4	0	3	1.97	3	265.4	−64,413	−4174	−512,476	0.83	−8.38	0.08	352.3	476.4	798.4	−1.47	1.16	87.1	31.6
27	Promazine	31.8	0	2	2.63	2	284.4	−65,321	−4185	501,582	2.89	−7.84	−0.24	461.7	508.8	860.3	−1.65	1.37	93.7	34.2
28	Phenytoin	58.2	2	4	2.48	4	252.3	−66,250	−3542	−454,910	2.86	−9.90	−0.39	333.5	435.7	716.5	−7.67	2.26	70.0	27.7
29	Hydroxyzine	35.9	1	4	2.00	4	374.9	−95,297	−5407	805,537	1.70	−9.13	−0.11	563.4	637.5	1092.8	−8.90	3.49	107.1	41.7
30	Mianserin	6.5	0	2	2.76	2	264.4	−63,761	−4290	−510,168	0.77	−8.46	0.20	365.6	479.6	808.8	−0.80	0.94	91.2	32.3
31	Valproic acid	37.3	1	2	0.16	2	144.2	−41,139	−2450	−216,934	4.47	−11.03	1.11	372.6	356.7	539.8	−4.39	2.61	40.3	16.2
32	Zopiclone	91.8	0	9	0.65	8	388.8	−102,536	−4710	−838,854	4.51	−9.36	−1.28	489.2	598.1	1025.2	−5.05	−1.83	101.9	37.9
33	Haloperidol	40.5	1	3	2.11	3	375.9	−100,303	−5164	−774,341	1.14	−9.12	−0.70	526.5	605.2	1035.8	−4.30	3.38	102.6	39.8
34	Risperidone	61.9	0	6	2.27	6	410.5	−111,074	−5964	−985,849	5.49	−8.87	−0.88	489.7	640.6	1127.2	−4.39	0.63	118.5	43.5
35	Loperamide	43.8	1	4	3.53	4	477.0	−119,284	−7065	−1,205,052	3.73	−8.93	−0.09	588.1	713.8	1308.0	−5.22	5.01	139.4	54.5
36	Phenylbutazone	40.6	0	4	0.10	4	308.4	−80,026	−4646	−632,151	0.90	−9.32	−0.26	473.7	543.9	920.5	−3.25	1.84	98.4	35.0
37	Clonidine	35.4	2	3	0.65	3	230.1	−53,612	−2372	−304,330	1.17	−8.96	−0.19	321.3	401.1	624.9	−5.73	0.28	62.2	22.7
38	PABA	63.3	3	3	−1.61	3	137.1	−38,905	−1859	−176,902	4.29	−8.50	−0.21	247.8	298.6	442.5	−11.00	0.96	37.5	14.3
39	Propylparaben	46.5	1	3	2.87	3	180.2	−51,913	−2627	−272,388	1.43	−9.52	−0.40	378.1	386.8	599.2	−7.99	2.30	48.6	19.1
40	Methylparaben	46.5	1	3	1.81	3	152.2	−45,017	−2067	−210,788	1.54	−9.53	−0.42	308.2	325.8	488.0	−9.09	1.49	39.3	15.5
41	Quetiapine	73.6	1	5	1.55	5	383.5	−95,297	−5413	−823,576	2.20	−8.64	−0.70	535.3	637.5	1098.9	−11.29	2.84	111.6	43.0
42	Chlorprotixen	28.5	0	1	4.40	1	315.9	−70,896	−4164	−520,729	1.94	−8.35	−0.56	510.5	545.8	912.1	−1.47	4.33	95.5	36.4
43	Perazine	35.0	0	3	3.13	3	339.5	−79,041	−5068	−693,691	2.18	−7.81	−0.17	453.1	550.9	986.5	−1.37	−0.76	114.4	40.3
44	Trifluoperazine	35.0	0	3	4.21	3	407.5	−111,907	−5402	−911,148	3.51	−8.19	−0.79	534.0	599.0	1067.0	−0.91	−0.19	119.7	41.8
45	Thioridazine	57.1	0	2	3.94	2	370.6	−82,689	−5253	−744,945	0.86	−7.78	−0.41	484.9	581.1	1039.3	−1.39	−0.42	123.0	43.8
46	Fluconazole	71.8	1	7	0.50	7	306.3	−89,231	−3607	−625,777	0.86	−10.43	−1.03	345.7	469.7	783.0	−10.28	−1.41	79.5	28.6
47	Tolperisone	20.3	0	2	2.27	2	245.4	−62,429	−4147	−464,977	2.97	−9.05	−0.15	436.5	486.1	815.0	1.41	3.01	79.6	29.5
48	Fenspiride	45.1	1	4	0.04	4	260.3	−69,140	−4020	−499,628	5.09	−9.28	0.16	401.1	475.0	791.6	−4.01	1.40	73.7	28.8
49	Pizotifen	31.5	0	1	4.49	1	295.4	−67,399	−4466	−549,282	1.15	−8.89	−0.32	379.1	505.1	869.1	−0.98	1.58	95.7	35.7
50	Cyproheptadine	3.2	0	1	4.86	1	287.4	−68,558	−4726	−566,080	1.04	−8.73	−0.36	378.9	516.5	887.5	−1.13	1.77	102.8	36.0
51	Closapine	30.9	1	4	0.76	4	326.8	−78,188	−4481	−629,966	3.11	−8.45	−0.61	433.0	545.3	926.1	−2.78	−0.73	103.5	36.5

Table 5. *Cont.*

		PSA	*HD*	*HA*	log *D*	*N+O*	M_W	E_T	E_b	E_e	*DM*	E_{HOMO}	E_{LUMO}	$S_a(a)$	$S_a(g)$	V_M	E_h	log *P*	*R*	α
52	Tiapride	84.1	1	6	−1.48	6	328.4	−88,376	−4474	−658,862	5.32	−9.27	−0.73	605.9	582.1	979.5	−5.66	−1.56	91.2	31.4
53	Olanzapine	59.1	1	4	2.68	4	312.4	−72,794	−4389	−594,188	3.31	−8.21	−0.72	437.2	534.2	901.5	−4.10	1.66	95.3	35.9
54	Betahistine	24.9	1	2	−2.18	2	136.2	−33,605	−2197	−176,624	2.59	−9.19	−0.05	328.2	351.2	521.3	−4.27	−0.52	46.0	16.6
55	Dexketoprofen	54.4	1	3	−0.25	3	254.3	−69,002	−3723	−449,051	1.60	−9.97	−0.57	402.6	470.1	768.0	−6.46	2.56	79.9	28.2
56	Caffeine	53.5	0	6	−0.13	6	194.2	−53,927	−2508	−319,054	3.78	−8.90	−0.49	341.4	365.3	572.9	−2.21	−1.06	50.0	18.9
57	Hymecromone	46.5	1	3	2.36	4	176.2	−50,477	−2397	−262,408	5.98	−9.21	−0.91	289.5	341.9	520.9	−9.80	−0.56	51.5	18.2
58	Ketotifen	48.6	0	2	3.28	2	309.4	−73,450	−4448	−586,056	4.06	−9.09	−0.97	389.1	508.1	876.7	−2.17	0.26	99.6	35.8
59	Clemastine	12.5	0	2	3.04	2	343.9	−84,433	−5152	−711,749	1.96	−8.95	−0.15	501.2	584.3	1012.5	−0.80	4.66	101.4	39.6
60	Salicylic acid	57.5	2	3	−1.06	3	138.1	−41,583	−1801	−184,688	0.99	−9.45	−0.60	236.5	284.1	420.5	−11.88	−0.04	38.6	13.7
61	Indomethacin	69.6	1	5	−0.16	5	357.8	−95,725	−4971	−704,963	2.36	−8.56	−0.61	509.6	562.9	961.3	−9.47	−1.43	103.3	36.7
62	Piroxicam	108.0	2	7	1.71	7	331.3	−88,167	−3947	−657,874	5.06	−8.99	−1.21	320.8	308.3	268.4	−11.67	−2.25	91.6	30.3
63	Naproxen	46.5	1	3	0.47	3	230.3	−63,546	−3396	−390,177	2.42	−8.67	−0.53	395.2	445.4	703.3	−9.53	0.56	70.6	25.3

4. Conclusions

This work has established that R_M/V_M is a useful descriptor of skin permeability derived from RP-18 thin layer chromatography. In a search for reliable log K_p models based on this descriptor two possibilities were considered: a relatively simple model based on 5 independent variables: (***N+O***), log ***D***, R_M/V_M, E_T and E_h (Equations (8) and (9)) and a more complex one, containing also E_b, M_W and ***PSA*** (Equations (10)–(12)). The latter accounts for over 90% of total variability and involves all the major properties that determine the drugs' ability to cross biological barriers (lipophilicity, molecular size, ability to form hydrogen bonds). It should be mentioned here that a very simple parameter (***N+O***) accounts for as much as 70% of the total log K_p variability; log ***D*** and R_M/V_M account for a further 10% and 5%, respectively.

Skin permeability is a difficult property to measure.Due to the limited availability of experimental permeability data for the solutes investigated in this study, the reference skin permeability coefficients were calculated according to a widely accepted model based on log P_{ow} and M_W (log K_p^{EPI}).

The advantages of this model are clear—it is based on easily obtained molecular properties, whose influence upon the skin permeability is well documented [21]. Of course, the reference model has also its limitations: it overestimates the results for very hydrophilic molecules [52,53], underestimates the values for non-hydrogen bonding solutes [52], and fails for extremely lipophilic compounds or solutes having a very high tendency to hydrogen bonding [18,53]. However, the group of solutes examined in this study does not include molecules of very high lipophilicity or with a very high tendency to H-bonding, and the differences between log K_p^{EPI} and log K_p^{exp} for hydrophilic solutes or non-H-bond donors are moderate. Small discrepancies between the calculated and experimental reference values (log K_p^{EPI} and log K_p^{exp}, respectively) for hydrophilic solutes or those without the H-donor sites may be a likely reason why the correlations between the experimental log K_p^{exp} values (where available) and the log K_p values calculated according to the equations developed in this study ((6), (8) and (10)) are better than those between log K_p^{exp} and log K_p^{EPI} for the same subgroup of compounds.

To conclude, Equations (6), (8) and (10) have been shown to be efficient tools for skin permeability predictions. Although Equation (10) provides the closest correlation, Equations (6) and (8) have the advantages of clarity and avoidance of colinearity between the variables; the simplest solutions are usually the best.

Author Contributions: Conceptualization, A.W.S.; methodology, A.W.S. and E.B.; investigation, A.W.S.; writing—original draft preparation, A.W.S.; revision—J.R. All authors have read and agreed to the published version of the manuscript.

Funding: This research was supported by an internal grant of the Medical University of Łódź no. 503/3-016-03/503-31-001.

Institutional Review Board Statement: Not applicable.

Informed Consent Statement: Not applicable.

Data Availability Statement: The data presented in this study are available in this manuscript.

Conflicts of Interest: The authors declare no conflict of interest. The funders had no role in the design of the study; in the collection, analyses, or interpretation of data; in the writing of the manuscript, or in the decision to publish the results.

Abbreviations

K_p—skin permeability coefficient; ***PSA***—polar surface area; ***D***—distribution coefficient; P_{ow}—octanol-water partition coefficient; M_w—molecular weight; M_{Pt}—melting point; H_b—total H-bond count; ***SsssCH***—sum of E-state indices for all methyl groups; ***ABSQon***—sum of absolute charges on nitrogen and oxygen atoms; ***A***—hydrogen bond acidity; ***B***—hydrogen bond basicity; ***S***—dipolar interactions; ***E***—excess molar refractivity; ***V***—McGowan's characteristic volume; H_d—H-bond donor activity;

H_a—H-bond acceptor activity; IAM—immobilized artificial membrane; BMC—biomedical chromatography; k—retention factor in column liquid chromatography; R_f—retention factor in TLC; TLC—thin layer chromatography; RP—reversed phase (chromatography); P_{mw}—micelle-water partitioning coefficient; k^{IAM} and k_{BMC}—retention factors in IAM and BMC chromatography, respectively; log ${k_w}^{IAM}$—log k^{IAM} measured at or extrapolated to purely aqueous conditions; Δlog ${k_w}^{IAM}$—the difference between log ${k_w}^{IAM}$ measured and predicted on the basis of log P_{ow}; V—McGowan's characteristic volume; K_{sc}—human skin-water partition coefficient; ***DM***—total dipole moment; V_M—van der Waals molar volume; $S_{a(a)}$—surface area (approximate); $S_{a(g)}$ –surface area (grid); E_{HOMO}—energy of the highest occupied molecular; E_{LUMO}—energy of the lowest unoccupied molecular orbital; E_T—total energy; E_b—binding energy; E_e—electronic energy; E_h—hydration energy; R—refractivity; α—polarizability; ***HD***—H-bond donor count; ***HA***—H-bond acceptor count; (***N+O***)—total nitrogen and oxygen atom count; ***Neoplastic-80***—antineoplastic-like property at 80% similarity; ***ALOGP***—log P_{ow} calculated using ALOGP algorithm; ***F06[C-N]***—frequency of carbon-nitrogen bond at a topological distance of 06; ***QXXp***—electrostatic interactions between electric quadrupoles of van der Waals forces; ${\pi_2}^H$—solute dipolarity/polarizability; $\Sigma{\alpha_2}^H$—solute overall hydrogen-bond acidity; ${\beta_2}^H$—solute overall hydrogen bond basicity.

References

1. Ng, K.W.; Lau, W.M. Skin Deep: The Basics of Human Skin Structure and Drug Penetration. *Percutaneous Penetration Enhanc. Chem. Methods Penetration Enhanc.* **2015**, 3–11. [CrossRef]
2. Todo, H. Transdermal Permeation of Drugs in Various Animal Species. *Pharmaceutics* **2017**, *9*, 33. [CrossRef]
3. Neupane, R.; Boddu, S.H.S.; Renukuntla, J.; Babu, R.J.; Tiwari, A.K. Alternatives to Biological Skin in Permeation Studies: Current Trends and Possibilities. *Pharmaceutics* **2020**, *12*, 152. [CrossRef]
4. El Tayar, N.; Tsai, R.-S.; Testa, B.; Carrupt, P.-A.; Hansch, C.; Leo, A. Percutaneous Penetration of Drugs: A Quantitative Structure–Permeability Relationship Study. *J. Pharm. Sci.* **1991**, *80*, 744–749. [CrossRef]
5. Anderson, B.D.; Raykar, P.V. Solute Structure-Permeability Relationships in Human Stratum Corneum. *J. Investig. Dermatol.* **1989**, *93*, 280–286. [CrossRef]
6. Potts, R.O.; Guy, R.H. Predicting Skin Permeability. *Pharm. Res.* **1992**, *09*, 663–669. [CrossRef]
7. Potts, R.O.; Guy, R.H. A Predictive Algorithm for Skin Permeability: The Effects of Molecular Size and Hydrogen Bond Activity. *Pharm. Res.* **1995**, *12*, 1628–1633. [CrossRef] [PubMed]
8. Barratt, M.D. Quantitative structure-activity relationships for skin permeability. *Toxicol. Vitr.* **1995**, *9*, 27–37. [CrossRef]
9. Neumann, D.; Kohlbacher, O.; Merkwirth, C.; Lengauer, T. A Fully Computational Model for Predicting Percutaneous Drug Absorption. *J. Chem. Inf. Modeling* **2006**, *46*, 424–429. [CrossRef]
10. Abraham, M.H.; Chadha, H.S.; Mitchell, R.C. The Factors that Influence Skin Penetration of Solutes. *J. Pharm. Pharmacol.* **1995**, *47*, 8–16. [CrossRef]
11. Abraham, M.H.; Martins, F.; Mitchell, R.C. Algorithms For Skin Permeability Using Hydrogen Bond Descriptors: The Problem of Steroids. *J. Pharm. Pharmacol.* **1997**, *49*, 858–865. [CrossRef]
12. Abraham, M.H.; Martins, F. Human Skin Permeation and Partition: General Linear Free-Energy Relationship Analyses. *J. Pharm. Sci.* **2004**, *93*, 1508–1523. [CrossRef] [PubMed]
13. Patel, H.; Berge, W.F.; Cronin, M.T.D. Quantitative structure–activity relationships (QSARs) for the prediction of skin permeation of exogenous chemicals. *Chemosphere* **2002**, *48*, 603–613. [CrossRef]
14. Chang, Y.-C.; Chen, C.-P.; Chen, C.-C. Predicting Skin Permeability of Chemical Substances using a Quantitative Structure-activity Relationship. *Procedia Eng.* **2012**, *45*, 875–879. [CrossRef]
15. Neely, B.J.; Madihally, S.V.; Robinson, R.L.; Gasem, K.A.M. Nonlinear Quantitative Structure-Property Relationship Modeling of Skin Permeation Coefficient. *J. Pharm. Sci.* **2009**, *98*, 4069–4084. [CrossRef]
16. Wilschut, A.; Berge, W.F.; Robinson, P.J.; McKone, T.E. Estimating skin permeation. The validation of five mathematical skin permeation models. *Chemosphere* **1995**, *30*, 1275–1296. [CrossRef]
17. Moss, G.P.; Dearden, J.C.; Patel, H.; Cronin, M.T.D. Quantitative structure–permeability relationships (QSPRs) for percutaneous absorption. *Toxicol. Vitr.* **2002**, *16*, 299–317. [CrossRef]
18. Mitragotri, S.; Anissimov, Y.G.; Bunge, A.L.; Frasch, H.F.; Guy, R.H.; Hadgraft, J.; Kasting, G.B.; Lane, M.E.; Roberts, M.S. Mathematical models of skin permeability: An overview. *Int. J. Pharm.* **2011**, *418*, 115–129. [CrossRef] [PubMed]
19. Fitzpatrick, D.; Corish, J.; Hayes, B. Modelling skin permeability in risk assessment—The future. *Chemosphere* **2004**, *55*, 1309–1314. [CrossRef]
20. Geinoz, S.; Guy, R.H.; Testa, B.; Carrupt, P.-A. Quantitative Structure-Permeation Relationships (QSPeRs) to Predict Skin Permeation: A Critical Evaluation. *Pharm. Res.* **2004**, *21*, 83–92. [CrossRef]
21. Lian, G.; Chen, L.; Han, L. An evaluation of mathematical models for predicting skin permeability. *J. Pharm. Sci.* **2008**, *97*, 584–598. [CrossRef] [PubMed]

22. Alonso, C.; Carrer, V.; Espinosa, S.; Zanuy, M.; Córdoba, M.; Vidal, B.; Domínguez, M.; Godessart, N.; Coderch, L.; Pont, M. Prediction of the skin permeability of topical drugs using in silico and in vitro models. *Eur. J. Pharm. Sci.* **2019**, *136*, 104945. [CrossRef]
23. Lien, E.J.; Gaot, H. QSAR Analysis of Skin Permeability of Various Drugs in Man as Compared to in Vivo and in Vitro Studies in Rodents. *Pharm. Res.* **1995**, *12*, 583–587. [CrossRef]
24. Chen, C.-P.; Chen, C.-C.; Huang, C.-W.; Chang, Y.-C. Evaluating Molecular Properties Involved in Transport of Small Molecules in Stratum Corneum: A Quantitative Structure-Activity Relationship for Skin Permeability. *Molecules* **2018**, *23*, 911. [CrossRef]
25. Mitragotri, S. A theoretical analysis of permeation of small hydrophobic solutes across the stratum corneum based on Scaled Particle Theory. *J. Pharm. Sci.* **2002**, *91*, 744–752. [CrossRef] [PubMed]
26. Sobańska, A.W. Application of planar chromatographic descriptors to the prediction of physicochemical properties and biological activity of compounds. *J. Liq. Chromatogr. Relat. Technol.* **2018**, *41*, 255–271. [CrossRef]
27. Sobańska, A.W.; Brzezińska, E. Phospholipid-based Immobilized Artificial Membrane (IAM) Chromatography: A PowerfulTool to Model Drug Distribution Processes. *Curr. Pharm. Des.* **2017**, *23*, 6784–6794. [CrossRef]
28. Sobańska, A.W.; Brzezińska, E. Application of planar and column micellar liquid chromatography to the prediction of physicochemical properties and biological activity of compounds. *J. Liq. Chromatogr. Relat. Technol.* **2019**, *42*, 227–237. [CrossRef]
29. Jevric, L.R.; Podunavac Kuzmanovic, S.O.; Svarc Gajic, J.V.; Kovacevic, S.; Jovanovic, B.Z. RP- HPTLC Retention Data in Correlation with the In-silico ADME Properties of a Series of s-triazine Derivatives. *Iran. J. Pharm. Res.* **2014**, *13*, 1203–1211. [CrossRef]
30. Kovačević, S.Z.; Jevrić, L.R.; Podunavac Kuzmanović, S.O.; Lončar, E.S. Prediction of In-silico ADME Properties of 1,2-O-Isopropylidene Aldohexose Derivatives. *Iran. J. Pharm. Res.* **2014**, *13*, 899–907.
31. Nasal, A.; Sznitowska, M.; Buciński, A.; Kaliszan, R. Hydrophobicity parameter from high-performance liquid chromatography on an immobilized artificial membrane column and its relationship to bioactivity. *J. Chromatogr. A* **1995**, *692*, 83–89. [CrossRef]
32. Barbato, F.; Cappello, B.; Miro, A.; La Rotonda, M.; Quaglia, F. Chromatographic indexes on immobilized artificial membranes for the prediction of transdermal transport of drugs. *II Farm.* **1998**, *53*, 655–661. [CrossRef]
33. Lázaro, E.; Ràfols, C.; Abraham, M.H.; Rosés, M. Chromatographic Estimation of Drug Disposition Properties by Means of Immobilized Artificial Membranes (IAM) and C18 Columns. *J. Med. Chem.* **2006**, *49*, 4861–4870. [CrossRef]
34. Hidalgo-Rodríguez, M.; Soriano-Meseguer, S.; Fuguet, E.; Ràfols, C.; Rosés, M. Evaluation of the suitability of chromatographic systems to predict human skin permeation of neutral compounds. *Eur. J. Pharm. Sci.* **2013**, *50*, 557–568. [CrossRef] [PubMed]
35. Soriano-Meseguer, S.; Fuguet, E.; Port, A.; Rosés, M. Estimation of skin permeation by liquid chromatography. *ADMET DMPK* **2018**, *6*, 140–152. [CrossRef]
36. Turowski, M.; Kaliszan, R. Keratin immobilized on silica as a new stationary phase for chromatographic modelling of skinpermeation. *J. Pharm. Biomed. Anal.* **1997**, *15*, 1325–1333. [CrossRef]
37. Martínez-Pla, J.J.; Martín-Biosca, Y.; Sagrado, S.; Villanueva-Camañas, R.M.; Medina-Hernández, M.J. Biopartitioning micellar chromatography to predict skin permeability. *Biomed. Chromatogr.* **2003**, *17*, 530–537. [CrossRef] [PubMed]
38. Martinez-Pla, J.; Martin-Biosca, Y.; Sagrado, S.; Villanueva-Camanas, R.; Medina-Hernandez, M. Evaluation of the pH effect of formulations on the skin permeability of drugs by biopartitioning micellar chromatography. *J. Chromatogr. A* **2004**, *1047*, 255–262. [CrossRef]
39. Waters, L.J.; Shahzad, Y.; Stephenson, J. Modelling skin permeability with micellar liquid chromatography. *Eur. J. Pharm. Sci.* **2013**, *50*, 335–340. [CrossRef]
40. Wang, Y.; Sun, J.; Liu, H.; Liu, J.; Zhang, L.; Liu, K.; He, Z. Predicting skin permeability using liposome electrokinetic chromatography. *Analyst* **2009**, *134*, 267–272. [CrossRef]
41. Seung Lim, J. EPI Suite: A Fascinate Predictive Tool for Estimating the Fates of Organic Contaminants. *J. Bioremediation Biodegrad.* **2016**. [CrossRef]
42. Bate-Smith, E.C.; Westall, R.G. Chromatographic behaviour and chemical structure I. Some naturally occurring phenolic substances. *Biochim. et Biophys. Acta* **1950**, *4*, 427–440. [CrossRef]
43. Soczewiński, E.; Wachtmeister, C.A. The relation between the composition of certain ternary two- phase solvent systems and RM values. *J. Chromatogr. A* **1962**, *7*, 311–320. [CrossRef]
44. Lipinski, C.A. Lead- and drug-like compounds: The rule-of-five revolution. *Drug Discov. Today Technol.* **2004**, *1*, 337–341. [CrossRef]
45. Veber, D.F.; Johnson, S.R.; Cheng, H.-Y.; Smith, B.R.; Ward, K.W.; Kopple, K.D. Molecular Properties That Influence the Oral Bioavailability of Drug Candidates. *J. Med. Chem.* **2002**, *45*, 2615–2623. [CrossRef] [PubMed]
46. Komsta, Ł.; Skibiński, R.; Berecka, A.; Gumieniczek, A.; Radkiewicz, B.; Radoń, M. Revisiting thin-layer chromatography as a lipophilicity determination tool—A comparative study on several techniques with a model solute set. *J. Pharm. Biomed. Anal.* **2010**, *53*, 911–918. [CrossRef]
47. Sobańska, A.W.; Wójcicka, K.; Brzezińska, E. Evaluation of the lipophilicity of selected sunscreens- A chemometric analysis of thin-layer chromatographic retention data. *J. Sep. Sci.* **2014**, *37*, 3074–3081. [CrossRef]
48. Sobańska, A.W.; Brzezińska, E. Application of RP-18 thin-layer chromatography and quantitative structure–activity relationship analysis for the prediction of the blood–brain barrier permeation. *JPC J. Planar Chromatogr. Mod. TLC* **2016**, *29*, 287–298. [CrossRef]

49. Sobańska, A.W.; Wanat, K.; Brzezińska, E. Prediction of the Blood-Brain Barrier Permeability Using RP-18 Thin Layer Chromatography. *Open Chem.* **2019**, *17*, 43–56. [CrossRef]
50. Pyzowski, J.; Brzezińska, E.; Sobańska, A.W. RP-18 chromatographic-based study of the blood—brain barrier permeability of selected sunscreens and preservatives. *JPC J. Planar Chromatogr. Mod. TLC* **2017**, *30*, 275–284. [CrossRef]
51. Geldenhuys, W.J.; Mohammad, A.S.; Adkins, C.E.; Lockman, P.R. Molecular determinants of blood–brain barrier permeation. *Ther. Deliv.* **2015**, *6*, 961–971. [CrossRef] [PubMed]
52. Fu, X.C.; Wang, G.P.; Wang, Y.F.; Liang, W.Q.; Yu, Q.S.; Chow, M.S.S. Limitations of Potts and Guy model and a predictive algorithm for skin permeability including the effects of hydrogen-bond on diffusivity. *Pharmazie* **2004**, *59*, 282–285. [PubMed]
53. Cronin, M.T.D.; Dearden, J.C.; Moss, G.P.; Murray-Dickson, G. Investigation of the mechanism of flux across human skin *in vitro* by quantitative structure-permeability relationships. *Eur. J. Pharm. Sci.* **1999**, *7*, 325–330. [CrossRef]